

# Indirect Method of Measurement and Evaluating the Noise Power Spectrum of A Medical X-ray Imaging System

Zeki Ahmed Darwish

National University of Malaysia (UKM)

Bangi 43600, Selangor, Malaysia

**Abstract**— The purpose of this paper is to estimate the noise power spectrum by autocorrelation function AFC using a different radiographic film and full field digital mammography. The autocorrelation function is a measure of similarity between a data set and a shifted copy data as a function of shift magnitude. This method has the advantage of providing the value of the noise power at zero frequency and the NPS calculated via autocorrelation function ACF is smoother than NPS, which is calculated by the direct fast Fourier method. Noise power spectrum computations using different images have been attempted using codes written in MATLAB® Version 7.8.0.347 (Math Works, 2009).

**Keywords**—Autocorrelation function; Noise power spectrum; Full field digital mammography. Fast Fourier Transform FFT

## I. INTRODUCTION

Noise is defined as undesirable image characteristics that reduce the visibility of specific objects. Any component of the signal that does not convey relevant information can be considered as noise [1]. Examples of noise are the fluctuations in the source signal, randomness in the detector output, and superimposed structures which are not related to the signal of interest. In general, image quality is determined by three primary physical parameters: contrast, spatial resolution and noise [2]. These quality parameters can be evaluated by objective image quality measurements such as signal-to-noise ratio (SNR), modulation transfer function (MTF) and Wiener spectra (WS). Together they form a basis for the description of image quality, which encompasses the three primary physical image quality parameters; (See Fig 1).

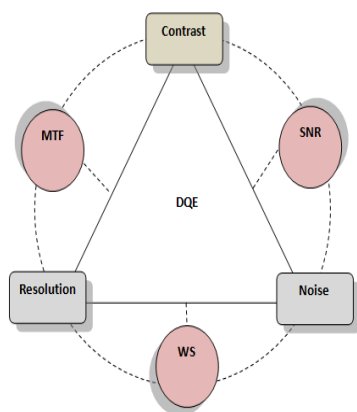


Fig.1 Image quality triangle: illustrates the Wiener spectrum in relation to parameters and physical image measurements [3].

With any imaging system, images are partially degraded by various sources of statistical fluctuation which arise along the imaging chain [4]. For example, quantum and electronic noise that produces random variations of signal can obscure useful information in a diagnostic image. Random noise means fluctuations of the signal over an image, as a result of uniform exposure, and can be characterized by the standard deviation of the signal variations over the image of a uniform object. The Wiener spectrum must be used to get a more complete description of the spatial correlation of noise: it measures noise power as a function of spatial frequency [4][5][6].

The noise power spectrum (NPS) of a radiographic film can be expressed in three constituent noise sources and can be written as

$$W_T(u) = W_Q(u) + W_G(u) + W_S(u) \quad (1)$$

where  $W_T, W_Q, W_G, W_S$  stand for the WS of the system radiographic noise, quantum mottle, film graininess and screen structure mottle respectively, and  $u$  is spatial frequency. Radiographic mottle is the fluctuations of film density from one area to another due to imaging system noise [7][8][9][10]. In order to specify the spatial structure of image noise or to describe any correlation between the densities at different points, the autocorrelation function of the fluctuation could be used [11].

Development in medical imaging systems has led to new sources of noise and new ways to address and minimize their impact on the quality of the image. As a digital detector, the measured noise power spectrum will suffer from aliasing because the noise data might have been sampled at discrete intervals by the pixel matrix. Williams et al (1999) discuss aliasing of NPS for digital mammography systems [12]. Detectors that produce images with significant spatial frequency content above the sampling limit prior to sampling will suffer from aliasing. Ultimately, aliasing leads to an increase in noise power at high spatial frequencies [13]. Some of the important theoretical aspects of noise power measurements are in the work of Cunningham [14,15] and Dobbins III (2000)[16].

The most economical way of estimating the autocorrelation for a given noise image is first to estimate the noise power spectrum and then calculate its inverse of fast Fourier (FT) [17]. Since the autocorrelation function may be calculated from the noise power spectrum, and vice versa, both of these methods provide equivalent and complete descriptions of the correlations present in the noise. In this study calculation of

WS via autocorrelation function offers significant advantages over the standard method by improving the accuracy with which the WS is determined and by allowing the NPS at zero frequency to be determined in a straightforward manner by using a radiograph film and full field digital mammography systems.

## II. BEUTEL'S METHOD

This method has the advantage of providing the value of the noise power at zero frequency and NPS calculated via autocorrelation function (ACF) is smoother than NPS, which is calculated by the direct (FT) method [18]. The formula for computing autocorrelation function (ACF) is

$$AFC(x_k) = \frac{1}{N^2} \sum_{K=0}^{N-1} \sum_{i=j=1}^N D_i D_{i+k,j} \quad (2)$$

A uniformly exposed radiograph is scanned by a microdensitometer, and optical density fluctuation data about the mean density is obtained by subtracting the mean density from the density values. Total  $N$  density values, each spaced by  $dx = 0.0125\text{mm}$  (sampling interval) are chosen. The density values  $D_i$  were low pass filtered to provide protection against aliasing. The first  $N$  points on the autocorrelation function are calculated using Equation 2.

## III. METHODOLOGY

The autocorrelation function is a measure of similarity between a data set and a shifted copy data as a function of shift magnitude. Correlation analysis is used to find periodic patterns in noisy data. The definition of autocorrelation function (ACF) is similar to that for the auto covariance function (ACVF). The auto covariance function estimator for record of  $N$  data point's  $x_i$  is given by

$$C_{xx}(k) = \frac{1}{N} \sum_{i=1}^{N-K} x_i \cdot x_{i+k} \quad (3)$$

That is, for a given shift (or lag) of the record along itself,  $k$ , the ACVF  $C_{xx}(k)$  is a summary of how well the shifted data resembles the unshifted record [17]. Noise power spectrum computations using different images have been attempted using codes written in MATLAB® Version 7.8.0.347 (Math Works, 2009). Fig2 shows the steps of calculating NPS by Matlab codes using different a radiograph film and full field digital mammography systems. In this work images A1.bmp and A3.bmp are digitized images obtained from analog images by scanning. The uniform background area of the film was scanned by a microdensitometer. This scanning gave image A1.bmp and A3.bmp. The size of the scan was  $1000 \times 1000$  pixels corresponding to the physical area of  $1.25\text{cm}$  by  $1.25\text{cm}$  and  $978 \times 590$  pixels corresponding to Images file0000.bmp, file0001.bmp and file0002.bmp are full field digital mammography systems. Images A1.bmp and A3.bmp were prepared at the Aberdeen Royal Infirmary, Scotland. Images file0000.bmp, file0001.bmp and file0002.bmp were prepared at Putrajaya Hospital, Malaysia.

## IV. RESULTS AND DISCUSSION

### A. Low Pass Filter

In Beutel's method, the data is low-pass filtered by averaging pairs of pixels; this is similar to the Wagner method. Using low pass filtering it was found that the noise power spectrum in the high frequencies is reduced as in Fig.3.

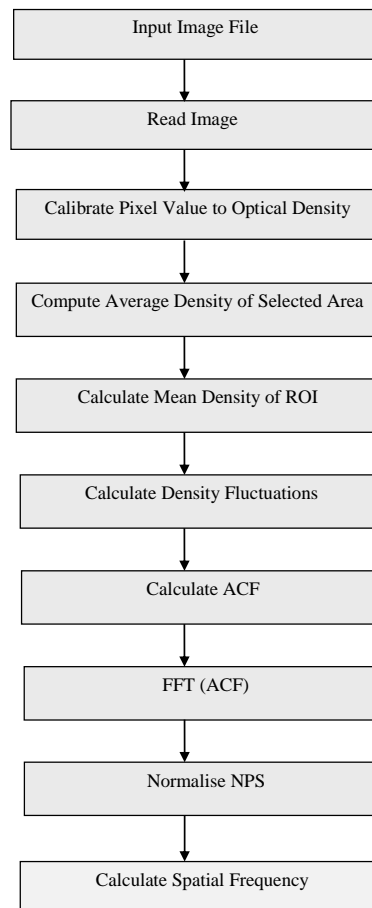


Fig2. Block diagram describes steps to compute the NPS by Beutel's method.

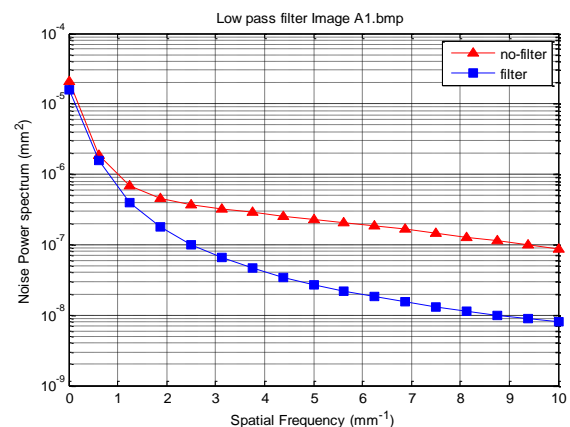


Fig. 3 NPS values were measured with low pass filter and without filter.

**B. Length of fast Fourier transform**

Fig.4 illustrates the effects of changing the fast Fourier transform FFT length (L) upon the NPS from different regions of interest ROI<sub>s</sub>. Table 1 shows different FFT segments. It was found that increasing FFT lengths caused a reduction of segment numbers and reduced the spatial frequency resolution without changing curve shapes.

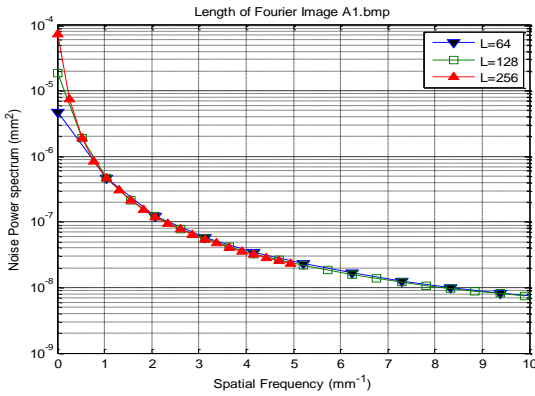


Fig. 4 Comparison among of NPS curves with different values of the length of Fourier transform

TABLE 1: Effect of fast Fourier transform length in the NPS curves in Fig. 4.

L	No of segments	Area (mm <sup>2</sup> )
64	255	1.527xe <sup>-005</sup>
128	49	3.021xe <sup>-005</sup>
256	9	6.008xe <sup>-005</sup>

**C. Data Shifting Factor K**

We conducted experiments to study NPS by changing the shifting factor *k* in Equation 2 on both digital (file 0000.bmp, file 0001.bmp) and analogue (A1.bmp, A3.bmp). We found that digital images give better results as shown in table 2, Fig.5 and Fig.6. After the change Equation 2 becomes as follows

$$AFC(x_k) = \frac{1}{N^2} \sum_{K=0}^{N-1} \sum_{i=j=1}^N D_{ij}D_{i,j+k} \tag{4}$$

Calculation of NPS by this equation was made using images A1.bmp and A3.bmp. It was found that there is no change in the NPS as in Fig.5 and Fig.6. For digital images (file0000.bmp, file0001.bmp) it was found that there is change as in Fig.7and Fig.8.

TABLE 2: Testing (k) factor used several different images.

Equation	$AFC(x_k) = \frac{1}{N^2} \sum_{K=0}^{N-1} \sum_{i=j=1}^N D_{ij}D_{i,j+k}$			
Image	Factor (k)	No. of segments	Area (mm <sup>2</sup> )	L
A1.bmp	(i+k, j)	49	3.0216e <sup>-005</sup>	128
A1.bmp	(i, j+k)	49	3.0216e <sup>-005</sup>	128
A3.bmp	(i, j+k)	28	3.0216e <sup>-005</sup>	128
A3.bmp	(i+k, j)	28	3.0216e <sup>-005</sup>	128
File0000.bmp	(i+k, j)	475	3.2851e <sup>-005</sup>	128
File0000.bmp	(i, j+k)	475	3.1708e <sup>-005</sup>	128
File0001.bmp	(i+k, j)	475	3.3508e <sup>-005</sup>	128
File0001.bmp	(i, j+k)	475	3.2103e <sup>-005</sup>	128

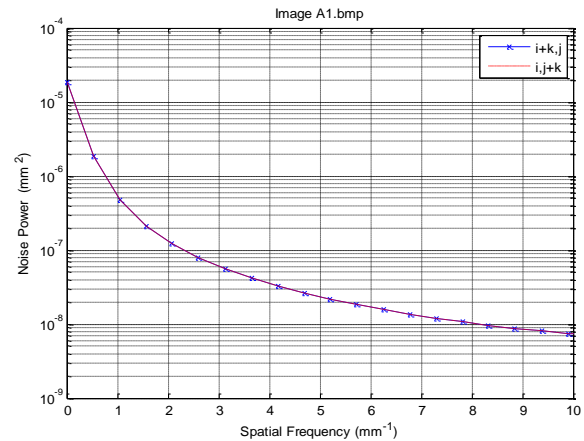


Fig.5 Comparison NPS values between two versions of factor (k) using image A1.bmp.

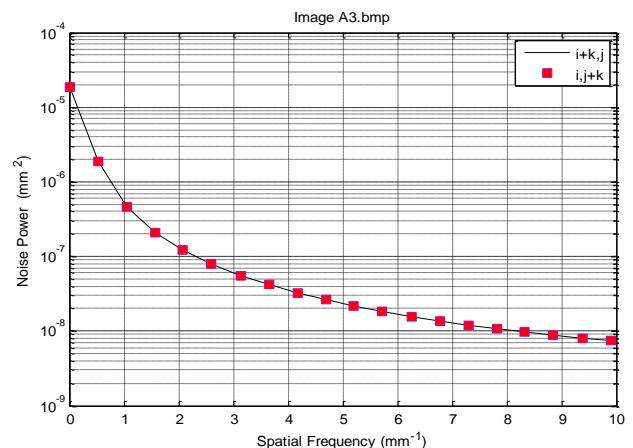


Fig.6 Comparison NPS values between two versions of factor (k) using image A3.bmp.

### III.CONCLUSION

In Beutel's method, the noise power spectrum was measured via autocorrelation function AFC. The AFC is a measure of similarity between data and shifted data as a function of shifted magnitude. The data was subjected to a low-pass filter by averaging pairs of pixels; this filter was based on Wagner's method. It was found that the NPS in the high frequencies is reduced. For the effects of changing fast Fourier length, it was found that increasing FFT length resulted in a reduction of segment numbers and a corresponding reduction in the spatial frequency resolution without changing curve shapes as presented in Table 1 and Fig. 4 respectively. We conducted experiments to study NPS by changing the shift factor  $k$  in Equation 2 on both digital and analogue images. We found that digital images give better results. The normalization of NPS was achieved by multiplying the square of the FFT with  $dx/L$  without using any windowing. It was found that the variance of density fluctuation equaled the area under the NPS curve and the order of magnitude of NPS obtained was  $10^{-3}$ - $10^{-5}$   $\text{mm}^2$ .

### ACKNOWLEDGMENT

The author would like to give great thanks to associate Prof. Dr. Wan Muhamad Saridan Wan Hassan the head department of physics Universiti Teknologi Malaysia for assistance to succeeding with this work. Finally, thanks go to Mr. Sultan Hasan Faleh at the Ministry of Education in the United Arab Emirates.

### REFERENCES

- [1] , R. S. Holland Fundamentals of radiographic Noise, . In A. G. Haus (Ed.), The Physics of Medical Imaging: Recoding Systems Measurements and Techniques (pp. 152-171.). New York,: American Assoc. of Physicists in Medicine 1979.
- [2] K. A. Jessen, "Balancing image quality and dose in diagnostic radiology," European Radiology Supplements, vol. 14, pp. 9-18, 2004.
- [3] D. Marsh and J. Malone, "Methods and materials for the measurement of subjective and objective measurements of image quality," Radiation protection dosimetry, vol. 94, pp. 37-42, 2001
- [4] J. T. Dobbins III, E. Samei, N. T. Ranger, and Y. Chen, "Intercomparison of methods for image quality characterization. II.Noise power spectrum)," Medical Physics, vol. 33, pp. 1466-1475, 2006.
- [5] Z. A. Darwish, A. Al Nassiri, W. M. S. W. Hassan, and H. Al Alawadhi, "The Method of Using slices to Estimate the Noise Power Spectrum of A Medical X-Ray Imaging System." International Journal of Engineering Research & Technology (IJERT), vol.4,p 736-743, 2015.
- [6] W. M. S. W. Hassan and Z. A. Darwish, "Comparison of Two Methods of Noise Power Spectrum Determinations of Medical Radiography Systems," in Malaysia Annual Physics Conference 2010 (PERFIK2010), 2011, pp. 321-323.
- [7] M. L. Giger, K. Doi, and C. E. Metz, "Investigation of basic imaging properties in digital radiography. 2. Noise Wiener spectrum," Medical physics, vol. 11, pp. 797-805, 1984.
- [8] W. Hassan, W. M. Saridan, Y. Munajat, and S. Sahibuddin, "Physical image quality evaluation of medical radiographs," Jurnal Fizik Malaysia, vol. 23, pp. 201-206, 2002.
- [9] K. Yoshiura, H. Stamatakis, U. Welander, W. McDavid, X. Shi, S. Ban, et al., "Physical evaluation of a system for direct digital intra-oral radiography based on a charge-coupled device," Dentomaxillofacial Radiology, vol. 28, pp. 277-283, 1999.
- [10] K. Doi, MTF's and Wiener Spectra of Radiographic Screen-film Systems, Volume II (including Speeds of Screens, Films and Screenfilm Systems): US Department of Health and Human Services, Public Health Service,

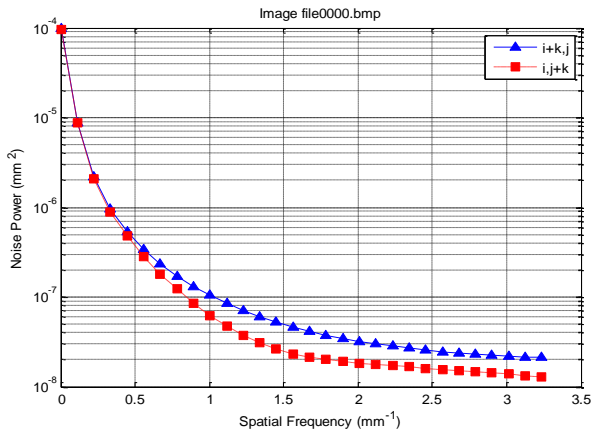


Fig. 7 Comparison NPS values of two versions of factor ( $k$ ) using image file 0000.bmp.

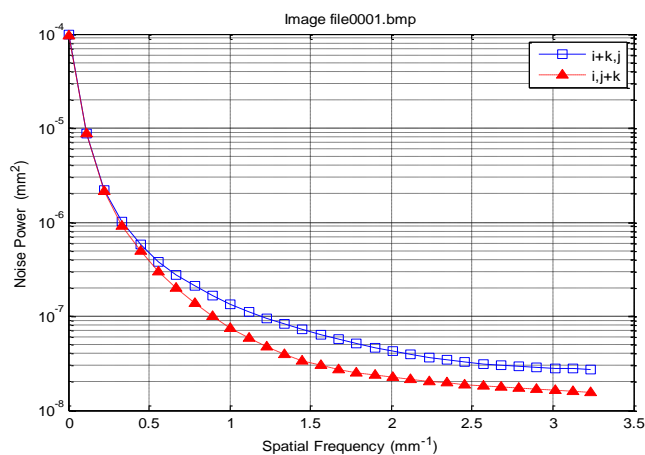


Fig.8 Comparison NPS values of two versions of factor ( $k$ ) using image file 0001.bmp.

### D. NORMALIZATION

In Beutel's method the normalization was reduce to  $dx/L$  without using any windowing. This was achieved by multiplying the square of the FFT with  $dx/L$ . As in Fig 9, when this normalization was used, we found the variance of density fluctuation equaled the area under the NPS curve and the order of magnitude of NPS obtained was  $10^{-3}$  to  $10^{-5}$   $\text{mm}^2$ . This result would be acceptable in practice.

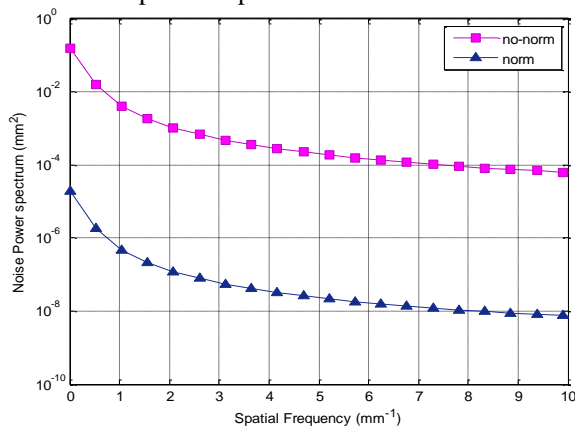
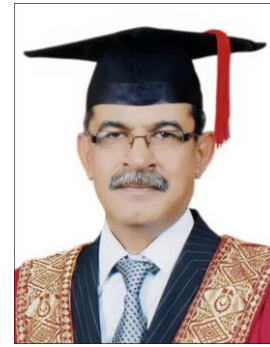


Fig. 9 Normalization the NPS measured via ACF.

Food and Drug Administration, Center for Devices and Radiological Health, 1986.

- [11] J. Miyahara, K. Takahashi, Y. Amemiya, N. Kamiya, and Y. Satow, "A new type of X-ray area detector utilizing laser stimulated luminescence," *Nuclear Instruments and Methods in Physics Research Section A: Accelerators, Spectrometers, Detectors and Associated Equipment*, vol. 246, pp. 572-578, 1986.
- [12] M. B. Williams, P. A. Mangiafico, and P. U. Simoni, "Noise power spectra of images from digital mammography detectors," *Medical physics*, vol. 26, pp. 1279-1293, 1999.
- [13] N. Marshall, "A comparison between objective and subjective image quality measurements for a full field digital mammography system," *Physics in medicine and biology*, vol. 51, p. 2441, 2006.
- [14] I. A. Cunningham. Image quality and dose. In J. A. Seibert, L. J. Filipow and K. P. Andriole (Eds.), *Practical Digital Imaging and PACS* (pp. 225-258), (1999). Madison, WI: Medical Physics Publishing Corporation,
- [15] I. A. Cunningham. Applied Linear-System Theory. In J. Beutel, H. L. Kundel and R. L. V. Metter (Eds.), *Handbook of Medical Imaging* (Vol. 1, pp. 79-162)(2000). Bellingham: SPIE.
- [16] J. T. Dobbins III. Image quality metrics for digital systems. In J. Beutel, H. L. Kundel and R. L. V. Metter (Eds.), *Handbook of Medical Imaging* (Vol. 1, pp. 161-222), (2000). Bellingham: SPIE Pubs.
- [17] R. F. Wagner, "Fast Fourier digital quantum mottle analysis with application to rare earth intensifying screen systems," *Medical physics*, vol. 4, pp. 157-162, 1977.
- [18] M. Beutel, Yampolsky, and R. Shaw, "Comparison of digital Wiener-spectrum calculation methods for screen-film evaluation," in *Medical Imaging*, pp. 320-329, 1993.

## BIOGRAPHIES



Zeki Ahmed Darwish received a BSc degree in Physics in 1984 Basrah University, Iraq and MSc degree in Physics from Universiti Teknologi Malaysia (UTM) in 2011. He is currently a PhD candidate at Solar Energy Research Institute, National University of Malaysia (UKM). Lecturer of Physics at Ministry of Education in United Arab Emirates. His research interests include Medical Imaging, Renewable Energy and Photovoltaic, Mathematical Modeling and Simulation by Matlab, Fuzzy logic controller and Artificial Neural Network (ANN).